

# Analysis of seismic noise in the Romanian-Bulgarian cross-border region

Bogdan Grecu  · Cristian Neagoe · Dragos Tataru · Felix Borleanu · Bogdan Zaharia

Received: 15 November 2016 / Accepted: 13 June 2018 / Published online: 20 July 2018  
© Springer Nature B.V. 2018

**Abstract** We present the first detailed investigation of the background seismic noise recorded in the Romanian-Bulgarian cross-border region over 3 years (2012–2015). We used the power spectral densities probability density functions (PSD PDFs) to study the noise variations in the period domain (0.025–1 s) as well as in the secondary microseism band (2–10 s). Strong diurnal variations and an increase of the noise levels during working days were observed at high frequencies at all stations, thus confirming the anthropic origin of the noise at low periods. The noise variations observed at longer periods ( $> 1$  s) are relatively small among the stations and are related to season changes. The dominant feature in the noise spectra between 2 and 10 s is the double-frequency peak (DFP) whose amplitude increases and changes during winter. For a specific interval, from 25th to 27th of January 2014, when a storm was reported in the Black Sea area, the maximum of the DFP shifted from larger periods ( $\sim 5.5$  s) at stations far from the Black Sea towards smaller periods ( $\sim 1.8$  s) at stations located on the coastline. The polarization analysis showed that the short period double-frequency microseisms originating from the Black Sea dominate during the winter month. Finally, we showed that site conditions vary due to noise variations related to weather conditions in the Black Sea or to changes in anthropogenic noise sources.

**Keywords** Seismic noise · Probability density functions · Diurnal and seasonal variations · Double-frequency peak · H/V ratios

## 1 Introduction

Ambient seismic noise represents those small amplitude ground vibrations that are permanently recorded on the surface of the Earth and generated by both anthropic and natural factors such as road traffic, industrial facilities, wind, oceanic and coastal waves, etc. These vibrations contaminate the seismic recordings and constitute a real inconvenience for the analysis of earthquake data. Therefore, seismic network operators usually try to reduce the seismic noise to provide high-quality data for seismological studies (e.g., seismic source and Earth structure investigations, microzonation and seismic hazard studies, etc.) as well as for data exchange between international seismological data centers.

However, in the last decades, benefitting from new research discoveries as well as from modernization of seismic stations and the development of dense seismic networks, the seismological community has started using seismic noise data in different disciplines and environments. Noise data became very important for estimating site effects in urban areas (Panou et al. 2005; Zaharia et al.

---

B. Grecu (✉) · C. Neagoe · D. Tataru · F. Borleanu · B. Zaharia  
National Institute for Earth Physics, Magurele, Romania  
e-mail: bgrecu@infp.ro

2008; Pilz et al. 2009; Cadet et al. 2011), investigating shallow (Boaga et al. 2010; Manea et al. 2016a, b), crustal and upper mantle structure (Shapiro et al. 2005; Yang et al. 2007; Saygin and Kennett 2008; Ren et al. 2013), understanding atmosphere-ocean-seafloor coupling (Kobayashi and Nishida 1998a, b), or climate changes (Stutzmann et al. 2009) as well as for studying the changes in the medium velocity or evidencing temporal physical changes in fault zones (Wegler and Sens-Schönfelder 2007; Brenguier et al. 2008). These latter studies represented may lead the work towards forecasting natural phenomena such as strong earthquakes and volcano eruptions, or monitoring changes in hydrocarbon reservoirs.

To help seismic network operators, researchers have developed useful tools for monitoring seismic station performance (e.g., McNamara and Buland 2004). They are based on the estimation of the background noise power spectral densities (PSD) and their probability density functions (PDF). They can be used to highlight problems in the operation of seismic stations and to identify those sites where the equipment has never worked or stopped working correctly. They also allow the estimation of the noise level at the seismic stations and its variations between day and night, different seasons of the year. Many studies took advantage of these

tools and used them to investigate the noise characteristics as recorded by different seismic networks: in USA (McNamara and Buland 2004), Italy (Marzorati and Bindi 2006), Spain (Diaz et al. 2010), Greece (Evangelidis and Melis 2012), New Zealand (Rastin et al. 2012), Romania (Greco et al. 2012), and Portugal (Custódio et al. 2014).

The seismic hazard of the cross-border region between Romania and Bulgaria is moderate to high (Dimitrova et al. 2015), mainly due to earthquakes occurring in four seismic zones that affect the area. Intermediate-depth earthquakes are generated in Vrancea region and crustal seismicity produced in the North and North-Eastern part of the Bulgarian territory (Gorna Orjahovitza, Dulovo, and Shabla). These seismic zones are capable of generating strong earthquakes with magnitudes larger than 7.0. In the last century, the study area was shaken by five major events, three of which occurred in Vrancea region (November 10th, 1940,  $M_w = 7.7$ ; March 4th, 1977,  $M_w = 7.4$ ; August 30th, 1986,  $M_w = 7.1$ ) (Oncescu et al. 1999), one in Shabla (March 31st, 1901,  $M_w = 7.1$ ), and one in Gorna Orjahovitza (June 14th, 1913,  $M_S = 7.0$ ) (Rangelov and Bojkova 2008) (Fig. 1). The event from Shabla generated a tsunami wave of 2–3 m height in the Black

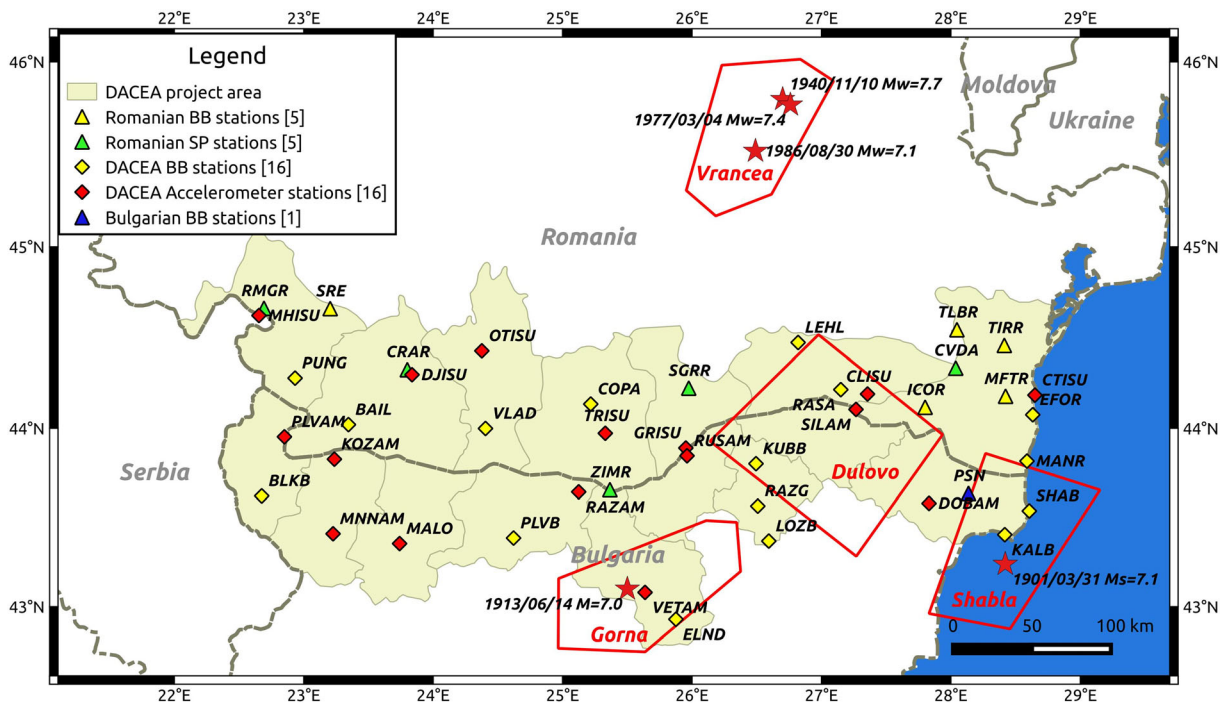


**Fig. 1** Map showing the seismic stations within the Romanian counties and Bulgarian municipalities. Earthquakes with magnitudes larger than 7.0 that affected the study area in the last century are plotted as red stars

Sea (Papadopoulos et al. 2011). The study region has also experienced a significant evolution in population growth and infrastructure development over the past century. The total population in the region is more than 5 million inhabitants. There are two nuclear power plants in the area, one in Romania (Cernavoda) and one in Bulgaria (Kozloduy), chemical plants located along the Danube river, the only bridge (motorway and highway) connecting Romania and Bulgaria, civil and military airports. To improve the quality of the earthquake database and the assessment of the seismic hazard in the cross-border region between Romania and Bulgaria, we must reduce the noise levels in the seismic data recorded by stations deployed in the area. The primary goal of our work is to study and understand the characteristics of the ambient seismic noise recorded at the permanent seismic stations located in the study area. After a description of the data and method used, we investigate the noise changes at low periods ( $< 1$  s) as well as in the secondary microseism band (2–10 s) for diurnal and seasonal variations. Polarization analysis in the period domain 2 to 10 s is performed to correlate the noise variations with weather conditions in the Black Sea. Finally, we also analyze the possibility of retrieving information about station site conditions by using the statistics of the power spectral density probability density functions.

## 2 Data and methods

Before 2010, the cross-border region between Romania and Bulgaria was characterized by a weak infrastructure for earthquake monitoring. This situation started improving in 2010, when a new project, Danube Cross-Border System for Earthquake Alert (DACEA), was launched by five partners from Romania and Bulgaria. The primary goal of the project was to develop an earthquake alert system. During the project, the monitoring infrastructure of the Romanian and Bulgarian seismic networks improved through the installation of 32 new seismic stations on both sides of the Danube River. Fifteen seismic stations have been installed in seven counties in the southern part of Romania, while 17 stations have been deployed in eight municipalities or counties in the northern region of Bulgaria (Fig. 1). Sixteen stations out of 32 are equipped with both broadband velocity (KS2000–120 s) and accelerometer (Episensor) sensors while the other stations only have

accelerometer sensors. The data recorded in all locations are transmitted in real-time to both Romanian and Bulgarian data centers.

The Romanian Seismic Network (RSN) operates as well five broadband (STS2–120 s, KS2000–100 s, CMG40T–30 s) and four short period (Marc Products L4C–1 s, Kinometrics S13–1 s, and SH1–1 s) real-time seismic stations (Fig. 1) in the DACEA project area. All of them are also equipped with accelerometer sensors (Episensor).

The noise analysis was carried out over a period of 3 years, from January 2013 till December 2015, for the sites with velocity sensors. We performed data quality checks to determine data gaps and availability for each station. We used the seismic channels with 100 sps, except for PSN station for which only data streams with 40 sps were available. Most Romanian stations have operated for the entire period analyzed, except some sites for which data became available after February 2013 (EFOR, CRAR, MFTR) or even March 2014 (TLBR). We used only five Bulgarian stations out of eight (ELND, KALB, PLVB, PSN, RAZG) due to the malfunctioning of the others.

To investigate the characteristics of the ambient seismic noise, we used the approach introduced by McNamara and Buland (2004). According to this study, the PDFs are computed for a large set of PSDs that are corrected in advance for the instrument response and converted to decibels with respect to acceleration. To facilitate the analysis and interpretation of the results, the spectral estimates are plotted together with two globally accepted standard models, Peterson's (1993) low and high new noise models (NLNM and NHHM). In most noise studies, signals such as earthquakes, calibration pulses, mass recenterers, spikes, etc., are regarded as 'unwanted signals' and usually are removed from the analysis. However, in this approach, these signals are considered to have a low probability of occurrence and do not contaminate the high-probability seismic noise observed in the PDFs and therefore are not removed from the computation of the PSDs. A complete portrayal of the method can be found in the work of McNamara and Buland (2004).

The background ambient seismic noise at each station was determined using SQLX software (Nanometrics) which is the commercial version of the open-source software package called PQLX (PASSCAL Quick Look eXtended) (McNamara and Boaz 2005). In Fig. 2, we present the noise PSD PDFs for the vertical

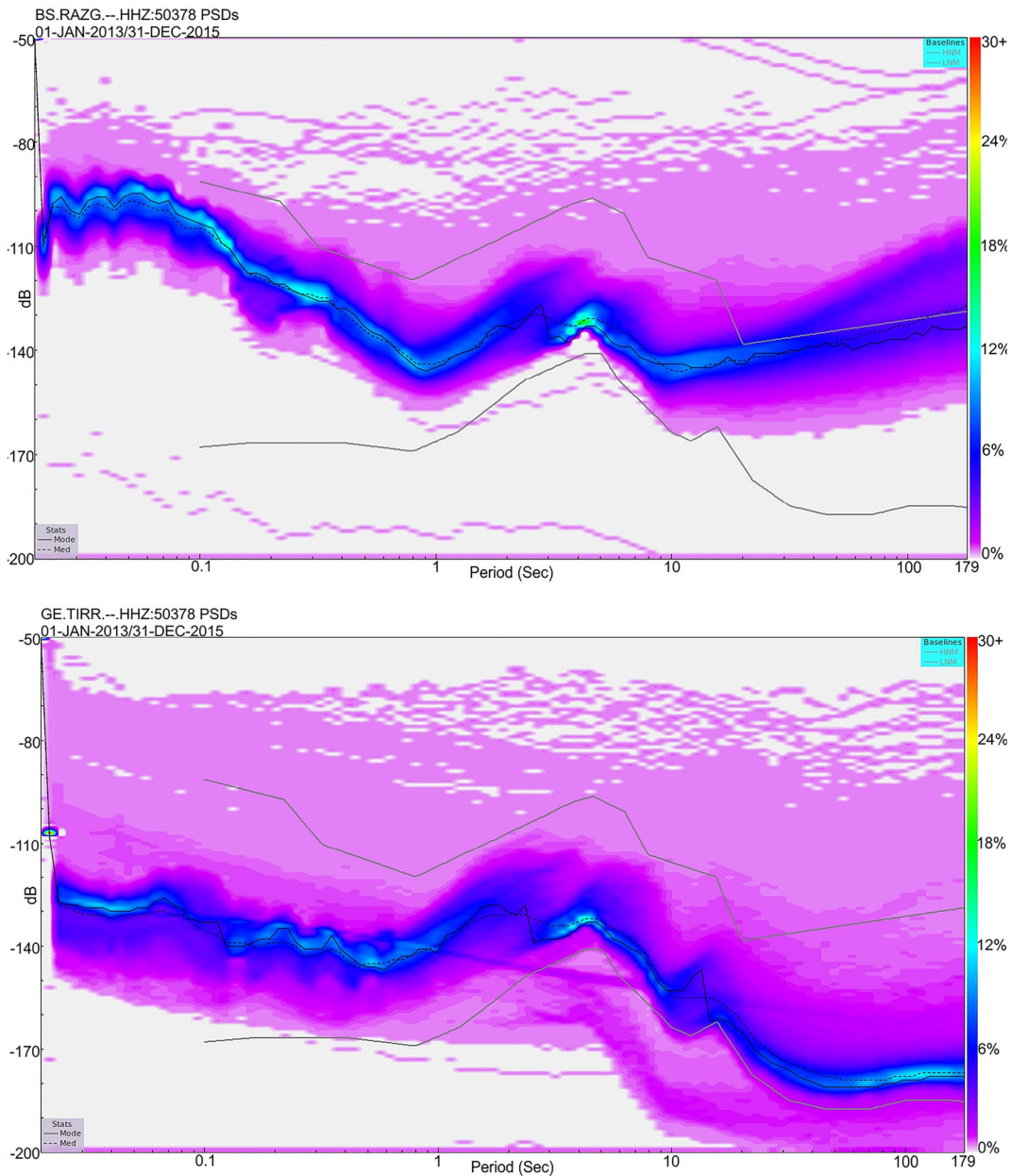


**Fig. 2** PSD PDFs for stations RAZG and TIRR (Z components) obtained using 45,237 and 50,378 PSDs during January 2013 to December 2015. Dashed and black lines are the median and mode of the PSD PDFs. The gray lines correspond to the NLNM and NHNM curves

components (HHZ) of two stations (TIRR and RAZG) obtained using SQLX. The lower probability PSDs correspond to the transient signals (e.g., earthquakes, calibration pulses, etc.) while the high-probability region depicts the background seismic noise level. At lower periods ( $< 1$  s), station TIRR shows lower background noise powers than station RAZG, while between 1 and 10 s, the level of seismic noise is similar. At larger

periods ( $> 10$  s), the high-probability region observed at station TIRR follows the NLNM very closely, whereas for station RAZG, it is closer to NHNM or even exceeds it. These differences are due to several factors such as anthropic noise sources at lower periods, seismic instrumentation, and station installation at larger periods. Station TIRR is equipped with STS2 velocity sensor with  $T_0 = 120$  s and has proper thermal isolation while

station RAZG is equipped with KS2000 velocity sensor with  $T_0 = 100$  s without an adequate thermal isolation. This behavior is outlined by the branch of the high-probability region that exceeds the NHHM for periods larger than 20 s and is obtained during colder months in winter (see station RAZG in Fig. 2). Due to these issues at long periods, we chose to limit our observations and analyses to periods below 10 s. For short period stations, this limit is set at 5 s.

Several statistics (min, max, mean, median, mode, etc.) of the PSD PDFs can be used to illustrate the distribution of observations. The mode of the PSD PDFs depicts better the background noise level at a given station, and it was used to compute new noise models for the USA (McNamara and Buland 2004) as well as for Greece (Evangelidis and Melis 2012). However, to make the comparison between stations much easier, Diaz et al. (2010) suggested using the statistical median of the PSD PDFs, as this curve is much smoother and does not split into two branches with similar probability. To have a better image of the differences between the noise levels at DACEA stations and implicitly on the stations' performance, we computed the median of PSD PDFs for each component of each station (Fig. 3). The most substantial difference in noise levels, reaching 60–70 dB, is noted for periods between 0.025 and 1 s for all components, while the lowest, reaching 25–35 dB, is observed for periods larger than 3 s. Also, at longer periods, one can notice an increase in the noise levels on the horizontal components compared to those observed on the vertical component. For several stations (BAIL, CVDA, EFOR, RMGR), the median of the PSD PDFs exceeds the NHHM for periods smaller than 1 s, while for station KALB (vertical component), the NHHM is surpassed between 0.6 and 2 s.

We also used noise data to extract information on station site conditions in terms of resonant effects. The horizontal to vertical spectral ratios of noise recordings (HVNSR) are sensitive to shear wave impedance contrast in the subsoil (Bard 1999) and provide the resonance frequency and an estimation of the lower limit level of the ground motion amplification of the site. We compute the HVNSRs following the standard approach described by the guidelines prepared by the SESAME project team (SESAME Project 2004) and using the statistics (median) of the PSD PDFs. In the first case, we used noise windows of 100 s length selected over the 3-day record and the Geopsy software ([www.geopsy.org](http://www.geopsy.org)) to compute the HVSRs. For the second case, the

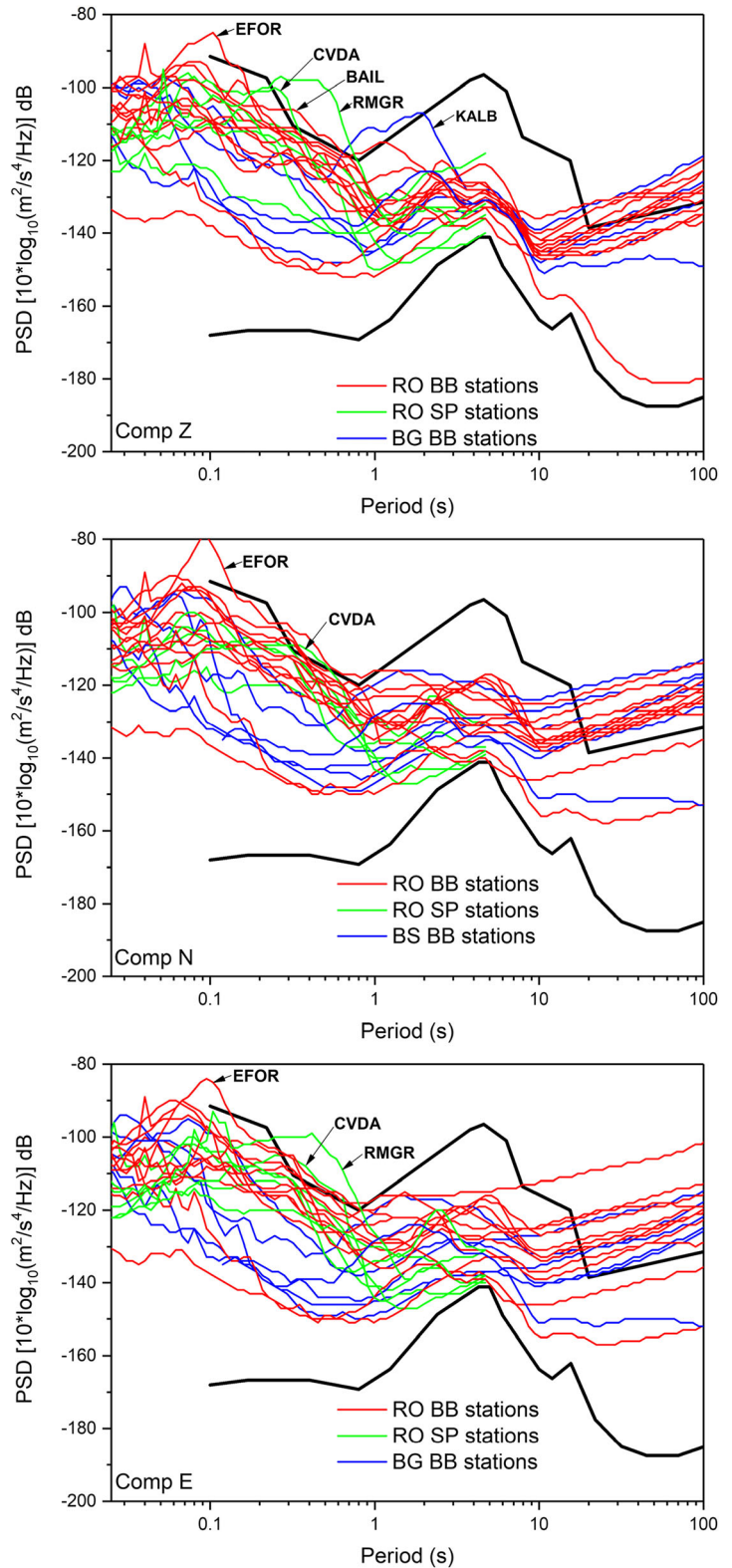
procedure consisted of the following steps: (i) we calculated the median of the PSD PDFs for each day over the selected period for each component of a station, (ii) we transformed the units of the median PSD PDF from dB to units of acceleration power spectral density according to Bormann (2012), (iii) we computed for each day the “horizontal component” by merging the PDF median of the EW and NS components using a geometric mean, and (iv) we divided the “horizontal component” by the vertical one (the median PDF computed for vertical component) without any smoothing. The procedure is very similar to the work of McNamara et al. (2014) who used the median of the PSD PDF to compute the horizontal-to-vertical spectral ratios in their investigation for the selection of a proper reference station needed for Q inversion. Also, in a recent study, Grecu et al. (2016) found a good agreement between the H/V ratios computed from noise data and median of the PSD PDF for stations in Bucharest area.

### 3 Noise variations

#### 3.1 Short period range (< 1 s)

The origin of seismic noise is of two types: natural and anthropogenic. At periods smaller than 2 s, seismic noise has both natural (wind, local running water) and anthropogenic origins. According to Kislov et al. (2010), wind may induce noise in seismic recordings due to changes in air pressure. Rivers produce ground vibrations in a wide frequency ranges due to collision of particles during sediment transport (Burtin et al. 2008). The dominant anthropic noise sources, such as power plants, factories, highways, etc., transmit energy into the Earth and generate most of the short period seismic noise. This type of noise shows significant diurnal variations related to the differences in the human activities between day and night. We computed the noise level variation for each hour of the day over 4 weeks (1st of September to 28th of September 2014) and the spectrogram for the same interval. Figure 4 shows the clear signature of the anthropogenic origin of the seismic noise in the period band 0.025–0.5 s. Its amplitude and the frequency band where is observed are different between stations. The spectrograms on the left panel of Fig. 4 outline the increase of the noise level during the working days as compared to the weekends, while the graphs on the right indicate

**Fig. 3** Median Power Spectral Density curves for all investigated stations: the red lines correspond to the Romanian broadband stations; the green lines correspond to Romanian short period stations and the blue ones correspond to the Bulgarian broadband stations. The black lines correspond to NHNM and NLNM



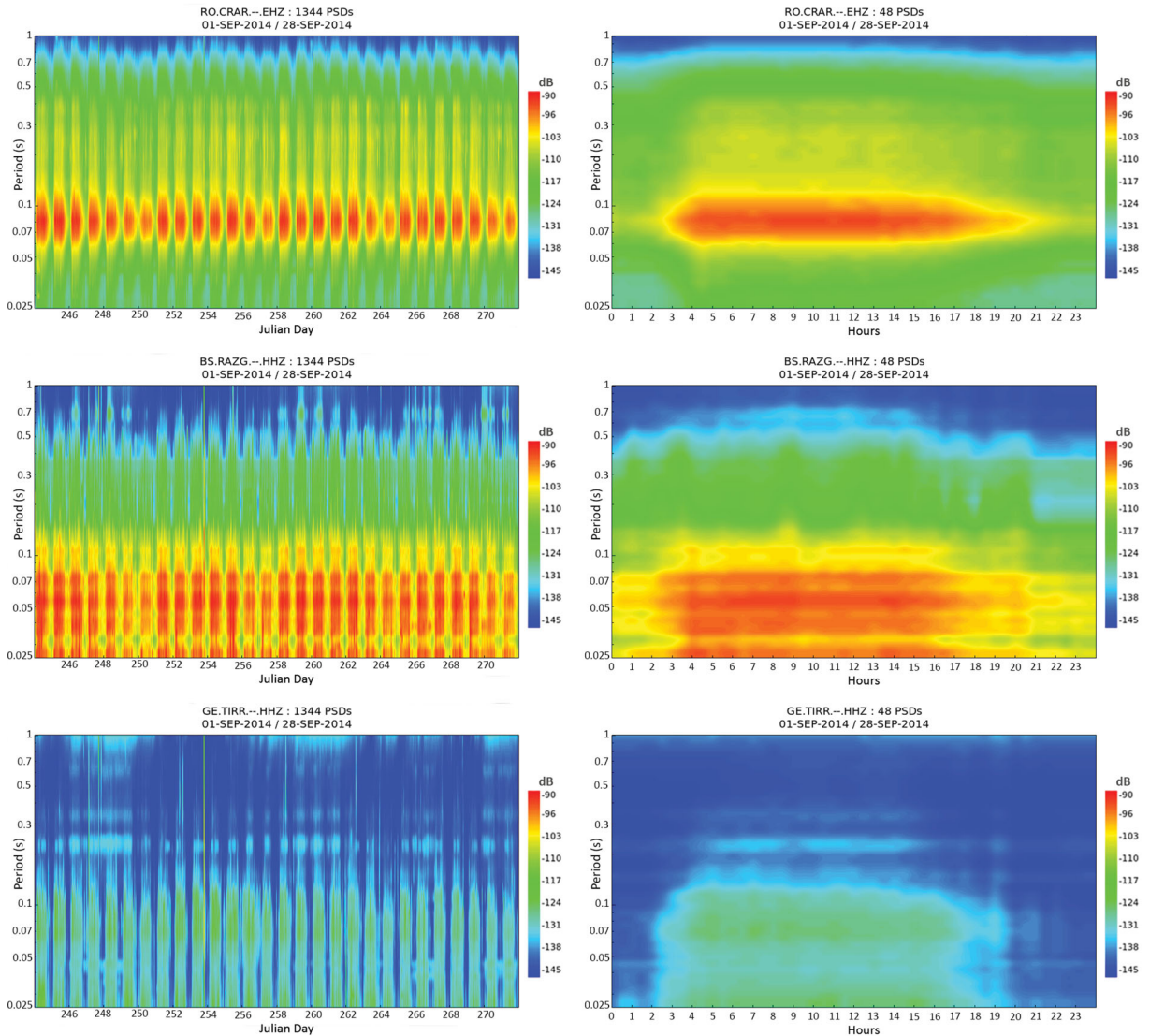


**Fig. 4** Anthropogenic signature of seismic noise in the domain 0.025–1 s observed at stations CRAR, RAZG, and TIRR. On the left, spectrograms of seismic noise computed between 1st and 28th

of September 2014 (days 244 and 272 correspond to Monday and, respectively, Sunday). On the right, spectrograms of seismic noise computed for each hour of the selected time interval

higher noise levels during day hours than during night hours. Stations within cities (CRAR) or close to an industrial zone near the Razgrad town (RAZG) in Bulgaria show higher noise levels than the noise level observed at station TIRR located farther south from a small village Targusor in Romania.

To map and quantify the diurnal variations at each station, we calculated the median of the PSD PDF for the vertical components in three period bands: 0.1–0.2 s (hereinafter referred as to band 1), 0.05–0.1 s (hereinafter referred as to band 2), and 0.025–0.05 s (hereinafter referred as to band 3). We considered two

intervals over the entire period of operation for each station, between 10 a.m. and 12 a.m. (GMT) for daytime and 00–02 a.m. (GMT) for nighttime, respectively. Next, following the same procedure as in Sheen et al. (2009) and Grecu et al. (2012), we computed the difference between daytime and nighttime noise level for each frequency band and we used the maximum of this difference for mapping. For each site, we represented a circle whose color indicates the nighttime median power level and whose size indicates the noise level differences between daytime and nighttime (Fig. 5). As expected, the results differ significantly

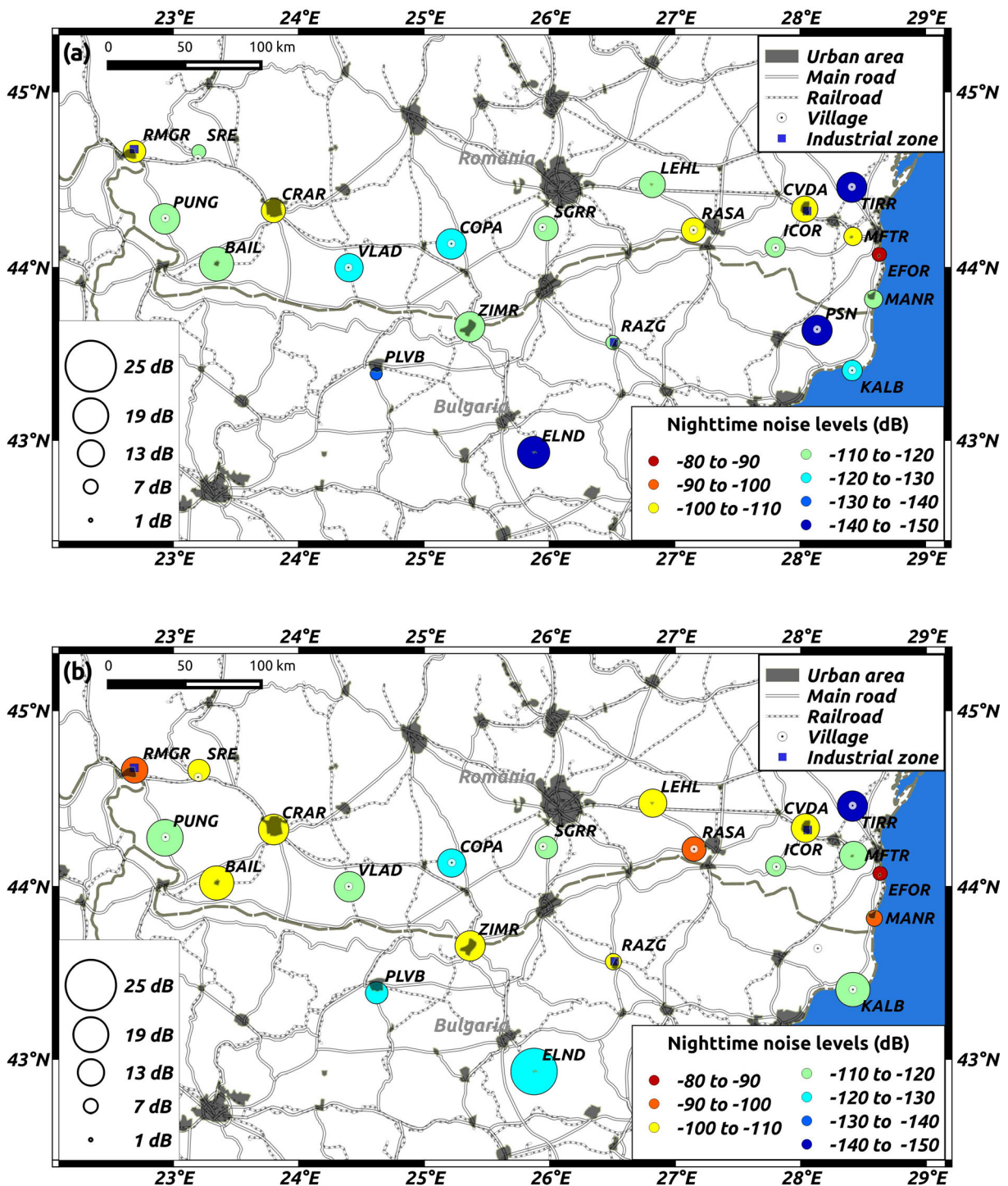


Fig. 5 Nighttime noise levels (colors) and noise level difference between daytime and nighttime (circles) in the selected period bands: a 0.1–0.2 s, b 0.05–0.1 s, and c 0.025–0.05 s

from one station to another. Since the noise sources in the short period band change from one site to another and the noise amplitude decreases rapidly with the

increasing distance from the sources, the noise variations are characteristic for each station. The maps in Fig. 5 do not represent a spatial distribution of the



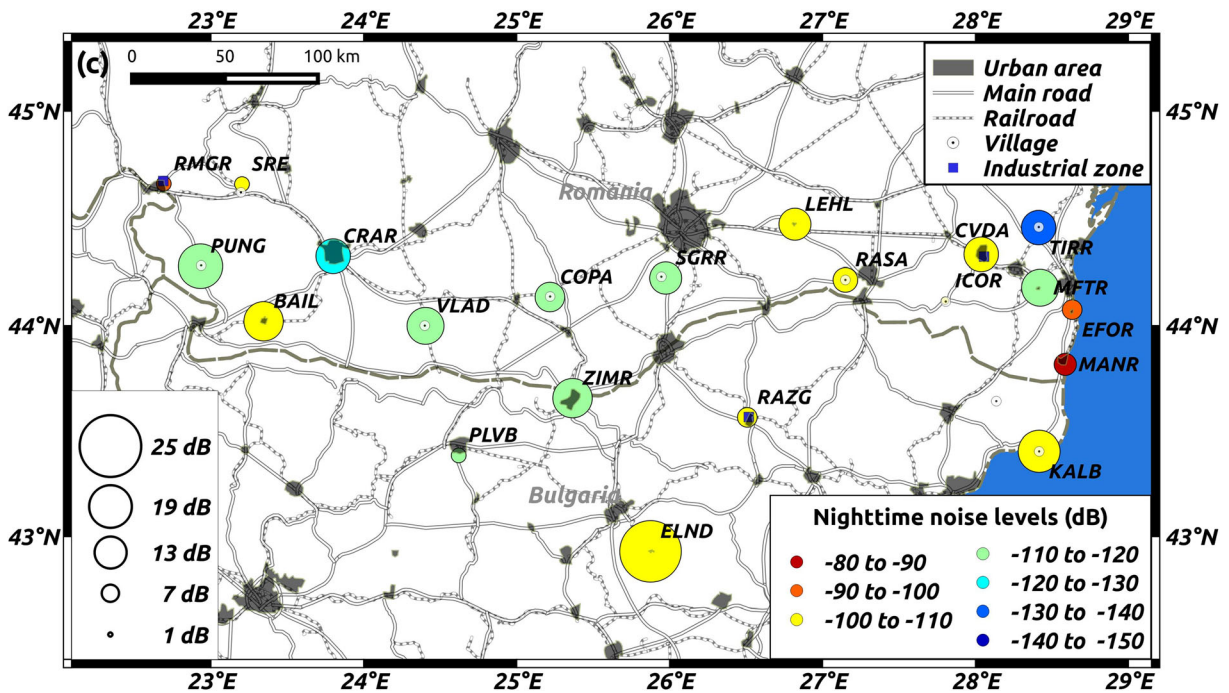


Fig. 5 (continued)

noise level across the studied area and we interpreted the results individually for each site. Most of the stations show important day-night variations. Station ICOR shows the smallest difference (3 dB), while station ELND shows the largest (25 dB), both observed in band 3. The nighttime noise levels seen at stations within cities (BAIL, CRAR, CVDA, EFOR, MANR, ZIMR) are in most cases larger than those observed at stations sited within villages (COPA, KALB, PUNG, SGRR, VLAD, TIRR). The noisiest stations found are EFOR and MANR for band 2 and band 3. They are located in two cities on the Black Sea coast, Eforie Nord and Mangalia, respectively. Besides the high nighttime noise level, they also show low day-night variations (< 9 dB). These observations indicate that these sites are permanently contaminated by important very local noise sources.

Two of the stations located close to industrial areas, RAZG and RMGR, have small day-night variations (7 dB) in band 3 and relatively high nighttime noise levels, between - 90 and - 110 dB. In band 2, RMGR shows an increase of the day-night noise level most likely due to the proximity of this station to a national road. As for the station CVDA, situated at about 2 km away from the Nuclear Power Plant Cernavoda, the noise sources generating the high-frequency noise seem

to be related to different sources within the city and not to the power plant. Figure 5 shows that the frequency band where the diurnal variations are largest is band 2. Almost all stations are close to primary or secondary roads, and therefore, the diurnal variations in this domain could be related to vehicular traffic.

The results presented in this section indicate that the performance of some stations (e.g., EFOR, MANR, RASA, RMGR) in the low period band (< 1 s) is strongly affected by important and permanent noise sources around the sites. Therefore, their capacity of recording small to moderate local earthquakes is reduced and network operators should take into consideration the possibility of relocating these stations.

### 3.2 Double-frequency microseism band

The domain between 2 and 10 s is named the double-frequency microseism band and the noise spectrum in this domain is characterized by a well-defined spectral peak, called double-frequency peak (DFP). DFP has natural origin and is generated when two oceanic waves of similar period traveling in opposite direction meet and produce standing gravity waves of half of the period of the ocean waves. Through a further nonlinear mechanism, the pressure excitation propagates to the

ocean floor where is coupled into elastic waves (Longuet-Higgins 1950). Taking into account the oceanic origin of the noise in this frequency band, many studies have shown a clear dependence of the noise levels with seasons (McNamara and Buland 2004; Marzorati and Bindi 2006; Diaz et al. 2010; Grecu et al. 2012; Evangelidis and Melis 2012; Rastin et al. 2012). To outline the presence of the noise seasonal variability in our dataset, we computed the noise level variation for each month of the year, for the available dataset at each station. Figure 6 shows the increase of the noise powers during winter between 2 and 9 s. It is interesting to note here the increase of the noise powers seen at stations LEHL and SRE in comparison with those observed at stations COPA and RAZG. However, the reason for this increase is also related to the thickness of the sediments beneath the stations and is discussed later in section 4.

To further investigate the seasonal variations, we also computed the median of the PSD PDFs for all the months of each season in the northern hemisphere. Figure 7 portrays the increase of the noise power levels in the DFP band during winter and the decrease of the noise levels during summer. It also indicates the

presence of two peaks between 2 and 10 s for the two stations (KALB, MANR) located in the coastal region of the Black Sea, one at lower periods ( $\sim 2$  s) and one at longer periods ( $\sim 7$  s). For the stations located farther from the Black Sea coast (RAZG, VLAD), a broader peak can be observed. Instead, the PUNG and SRE stations exhibit only one peak which broadens towards longer periods from summer to winter. It is worth noting here that station PUNG also shows seasonal variations for lower periods. The PUNG site is located at the edge of a village closer to agricultural land; therefore, the noise sources at these periods are most probably generated by agricultural activities which are low during winter time.

Bromirski et al. (2005) observed the splitting of the DFP into two peaks, one at short periods (SPDF) and one at long periods (LPDF). In a recent study, Beucler et al. (2015) investigated the microseisms generated in the North Atlantic and showed that the noise in the short period (2.5–5 s) is generated in the open sea, while the coastal region produces secondary microseisms in the period range (2.5–10 s).

To explore more the observed splitting of the DFP, we selected four stations located at different distances

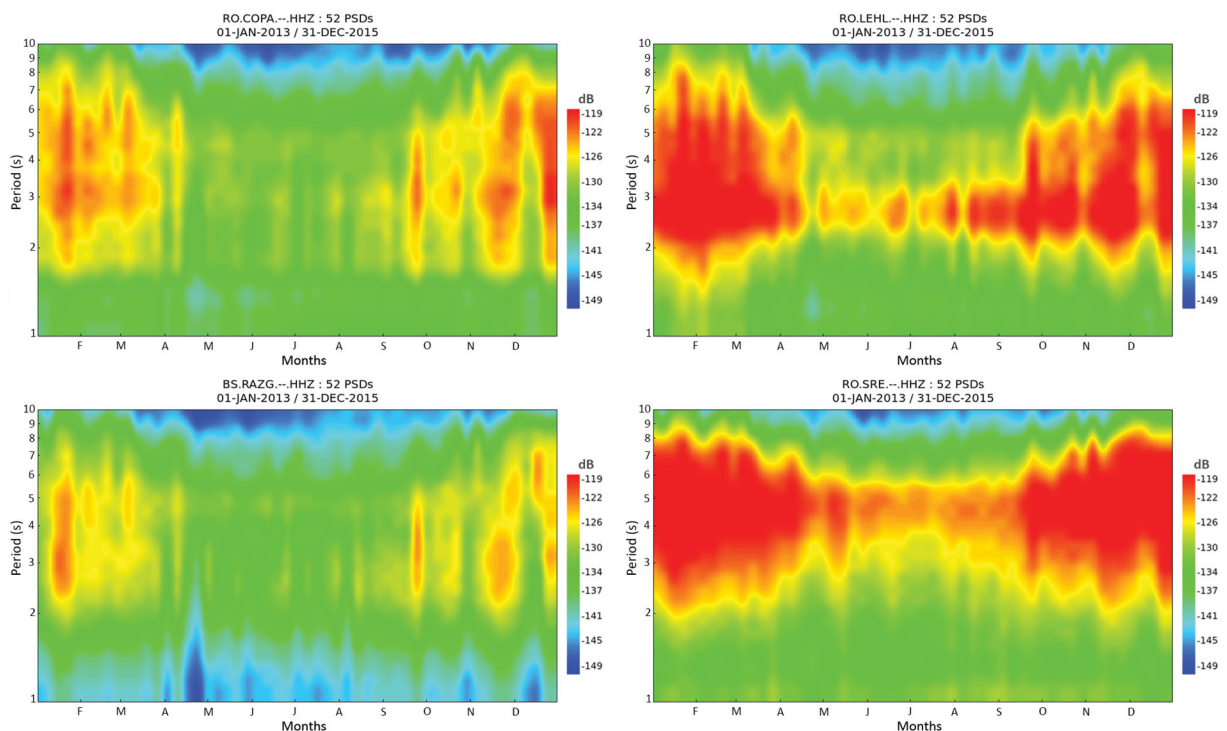


**Fig. 6** Seasonal variations for stations COPA, LEHL, RAZG, and SRE. The spectrograms outline the increase of the noise power levels from October to April in the 2–9 s band

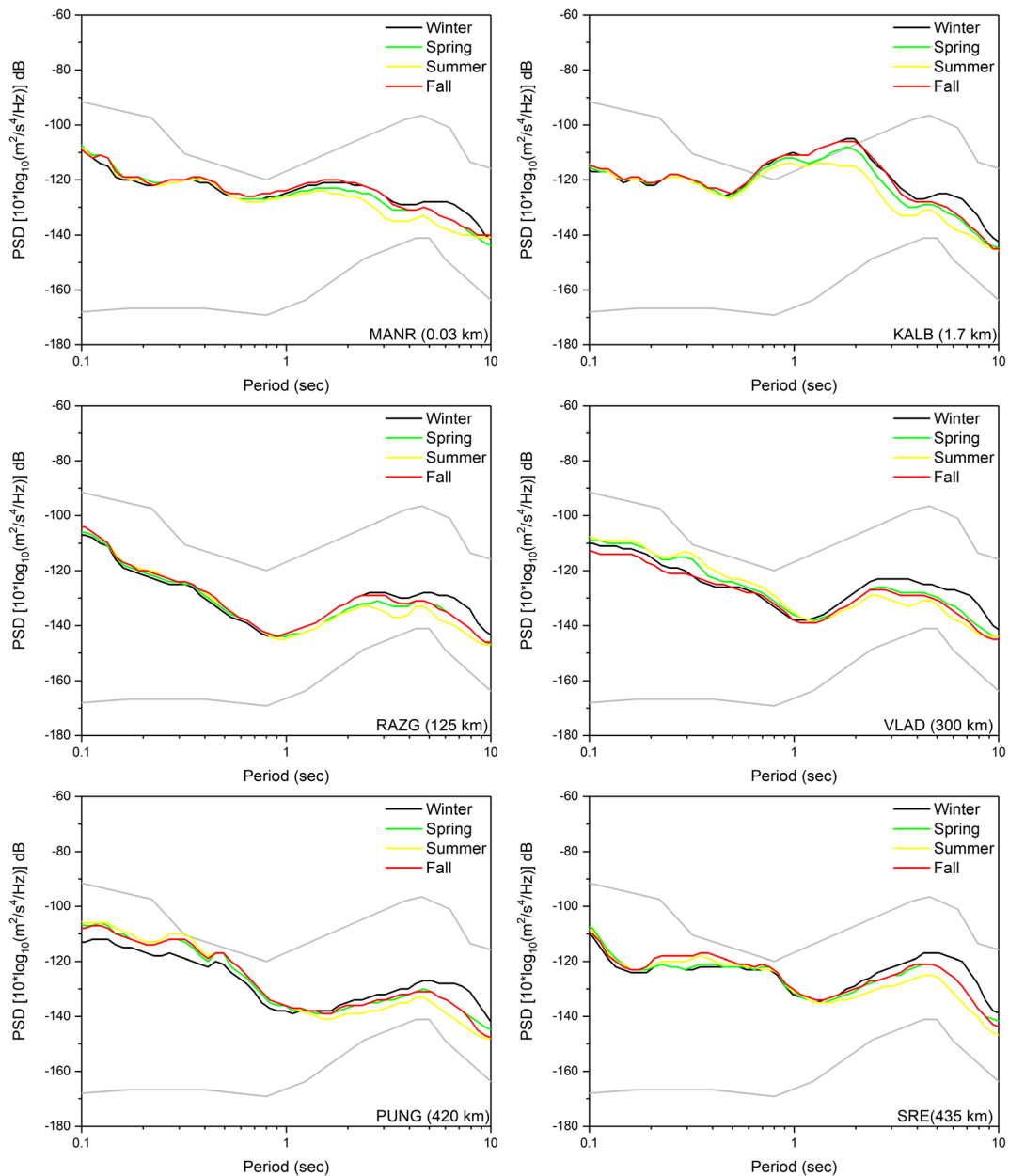


**Fig. 7** Median of the PSD PDFs at stations KALB, MANR, RAZG, VLAD, PUNG, and SRE computed for 3 months intervals, from January 2013 to November 2015

from the Black Sea coastline (MANR, RAZG, SRE, and TIRR) and data for two intervals with varying weather conditions. The first one between 24th and 28th of January 2014 when a storm hit the Black Sea area (Chiotoroiu et al. 2014) and the second one between 10th and 14th of August, without storms. For each interval, we computed the spectrograms for the vertical components (Fig. 8a) and found a significant increase of

the noise level in the DFP band (~2–10 s) during the winter days as compared to the summer days. Furthermore, we computed the median of the PSD PDFs for the time interval where we observed the burst of the noise powers (i.e., between 25th and 27th of January 2014) as well as for the ‘quiet’ summer period (i.e., 11th and 13th of August 2014) (Fig. 8b). During the stormy winter days, all stations show an increase of the noise powers

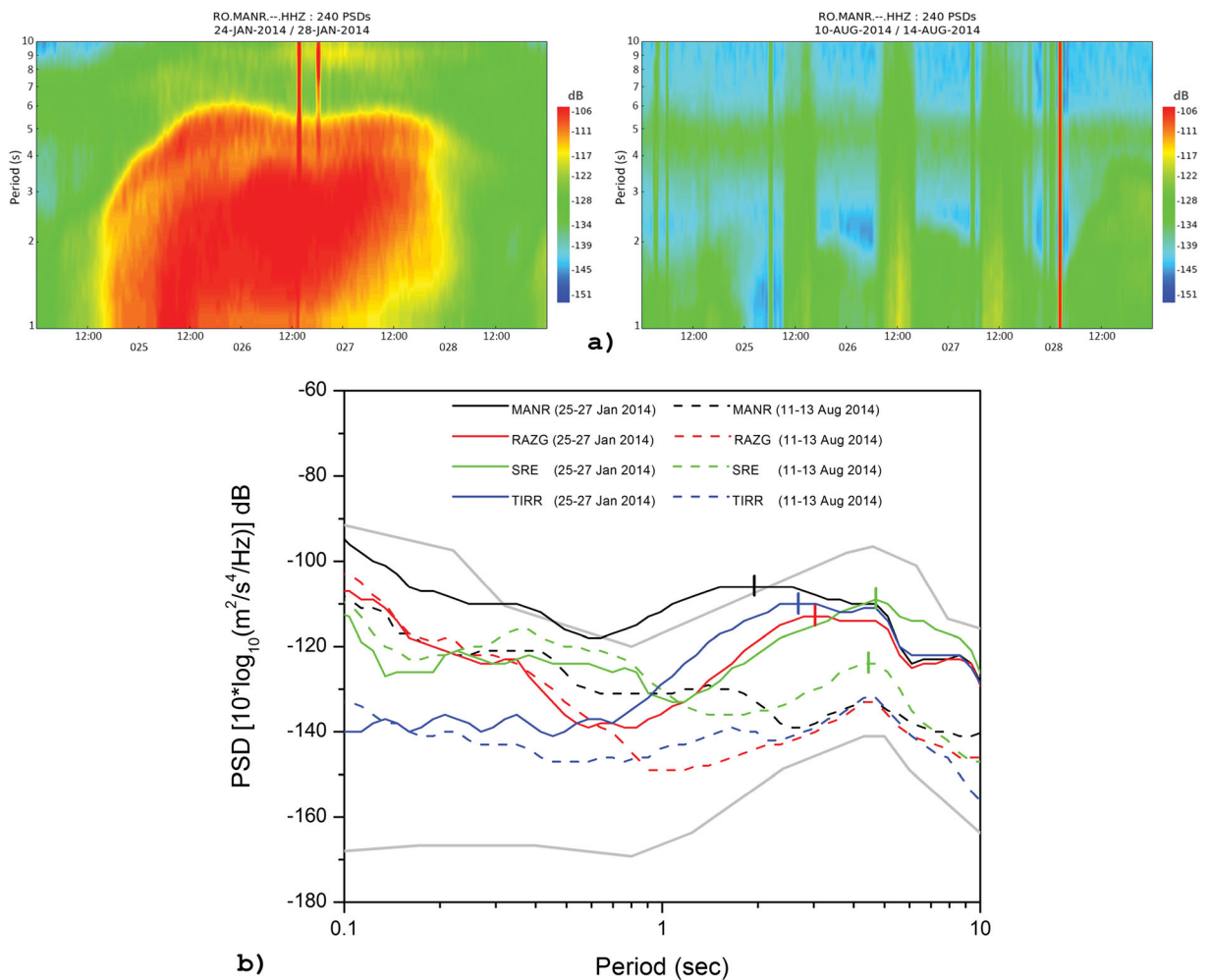


**Fig. 8** **a** Spectrograms computed for the vertical component of station MANR for the interval 24–28th of January 2014 (left) and 10–14th of August 2014 (right). Note the increase of the noise level in the period band 2–10 s during the winter time. **b** Median of

the PSD PDFs at stations MANR, RAZG, SRE, and TIRR computed for the winter interval (25–27th of January 2014) and the summer interval (11–13th of August 2014). The small vertical lines help to outline the shift of the DFP

up to 27 dB in comparison with the noise powers computed for the summer days. Also, the stations closer to the Black Sea coastline (MANR, TIRR, RAZG) exhibit a split and shift of the DFP peak towards shorter periods for the colder interval. This shift is more pronounced for stations closer to the shoreline. Instead, for the station located farthest from the Black Sea coastline (SRE), the DFP peak shows a small shift from approximately 4.3 to 4.7 s from summer to winter. The DFP shift could be related to the different regions of microseisms generation and is investigated through the polarization analysis performed at the stations.

In the absence of seismic arrays, polarization analysis of seismic noise represents an alternative for

constraining the incoming direction of microseisms at a particular station (Schulte-Pelkum et al. 2004; Chevrot et al. 2007; Stutzmann et al. 2009; Schimmel et al. 2011). We performed this analysis for stations BAIL, MANR, PSN, RAZG, SRE, and TIRR on the continuous records selected over two different months, January 2014 and August 2014, respectively. The polarization analysis is performed in the time-frequency domain (Schimmel et al. 2011) for two bands corresponding to the SPDF (2–4 s) and LPDF (4–10 s). This method has the advantage of using shorter time windows compared to the time domain covariance approach (Schulte-Pelkum et al. 2004) and is also better suited for the analysis of multiple sources

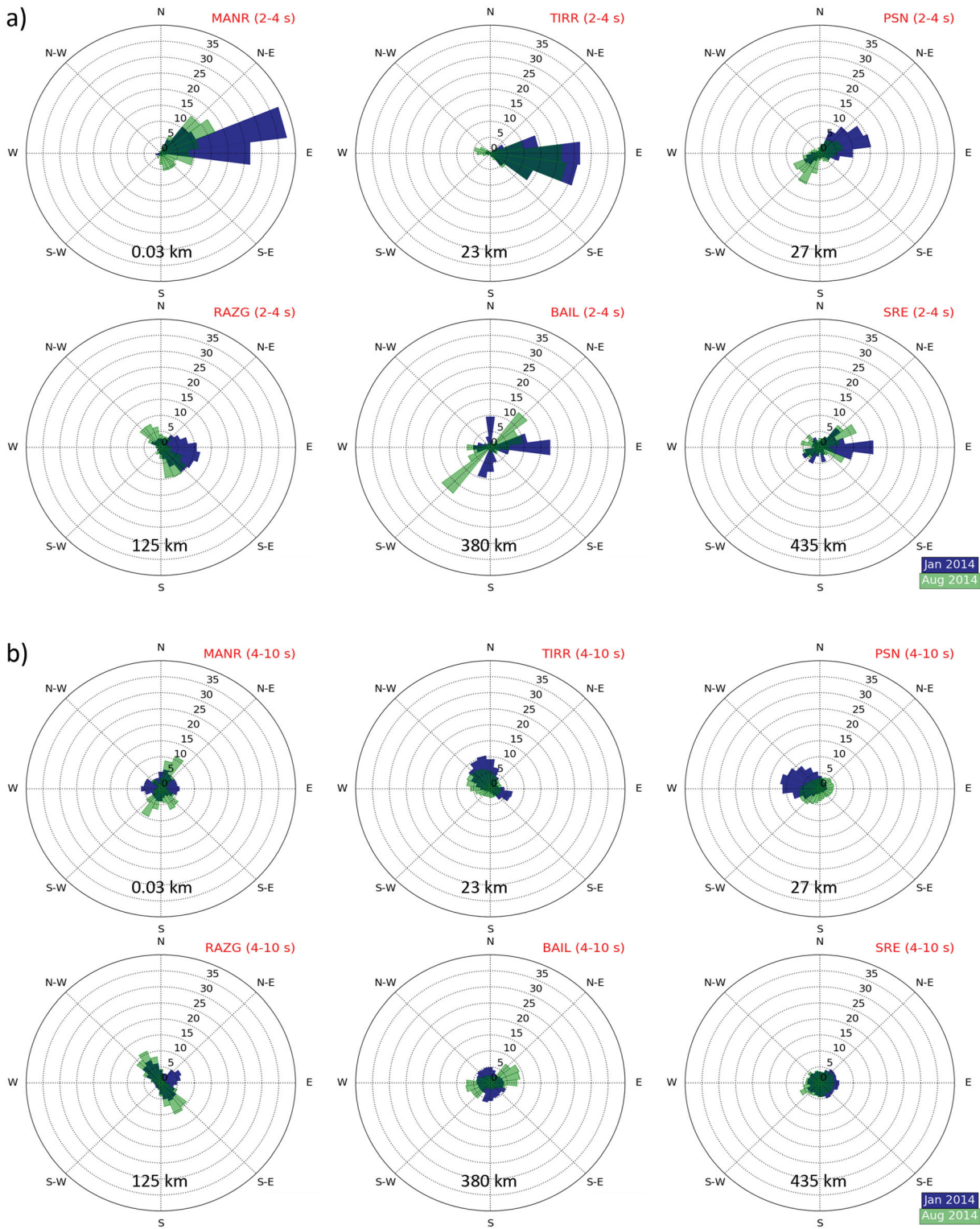


**Fig. 9** Rose diagrams with station particle motion back azimuths in the microseismic band **a** 2–4 s and **b** 4–10s obtained from noise data recorded during

of the seismic noise. The time-frequency approach measures the degree of polarization of the seismic noise in the microseisms band and focuses on the elliptically polarized signals. These signals are characteristic of Rayleigh waves and are found in a significant proportion in the microseisms. We present the results of the polarization analysis in terms of back azimuths (BAZ) which express the directions of the incoming waves. We considered in our study only the signals having a degree of elliptical polarization greater than 0.75 (1 indicating a perfect polarized signal of elliptical particle motion in a vertical plane, Schimmel et al. 2011). Figure 9 shows the back-azimuths compiled in normed stacked angular histograms. The main directions observed in the period domain 2 to 4 s point towards the Black Sea in winter and dominate for stations closer to the coastline (MANR, TIRR, PSN, RAZG). The stations located more inland (BAIL, SRE) also show directions pointing to the Mediterranean Sea (Fig. 9a). When analyzing the summer period, we can notice some overlapping of the main directions with those observed for winter ( $35^{\circ}$ – $95^{\circ}$  for MANR,  $45^{\circ}$ – $90^{\circ}$  for PSN,  $110^{\circ}$ – $170^{\circ}$  for RAZG,  $70^{\circ}$ – $130^{\circ}$  for TIRR). Stations BAIL, PSN, and SRE also show azimuths pointing to the Mediterranean Sea ( $220^{\circ}$ – $260^{\circ}$  for BAIL,  $205^{\circ}$ – $250^{\circ}$  for PSN,  $220^{\circ}$ – $265^{\circ}$  for SRE) (Fig. 9a). For the longer periods (4–10 s), the BAZs are relatively homogeneous between winter and summer for the same station (Fig. 9b), suggesting that the noise sources are more uniformly distributed around the stations. Furthermore, the directions toward the Black Sea do not dominate the histograms anymore although they are present for most of the stations. The polarization analysis allowed us to conclude that the Black Sea represents an important area of noise sources in the SPDF domain for the stations located in the study area.

#### 4 Influence of the noise variations on site conditions

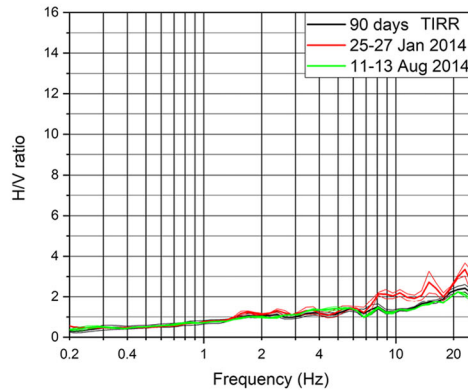
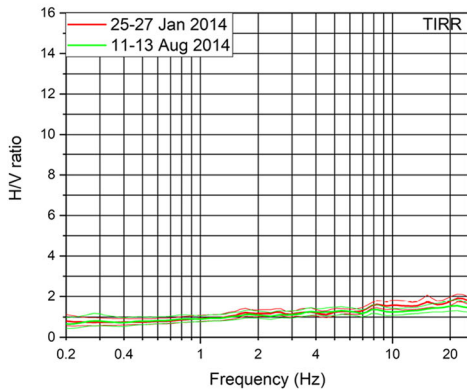
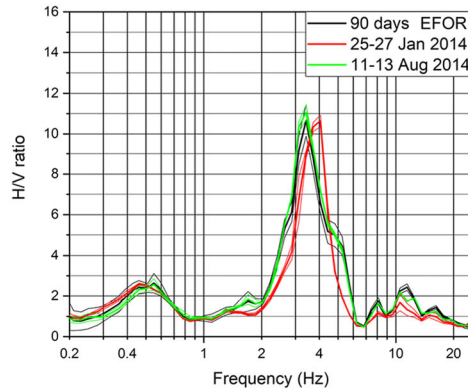
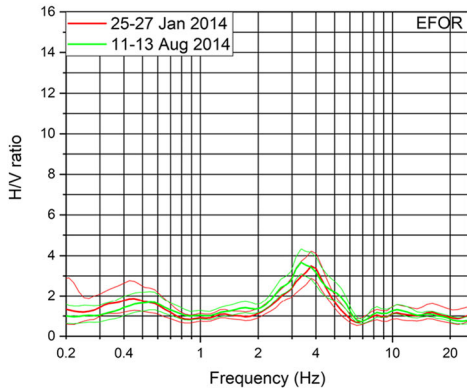
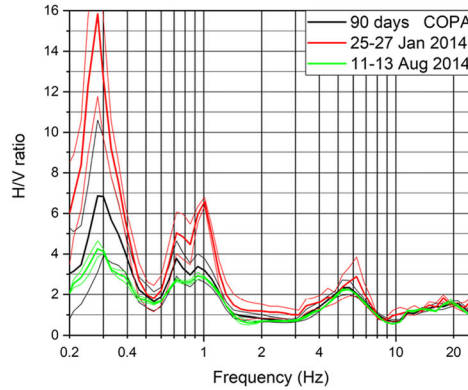
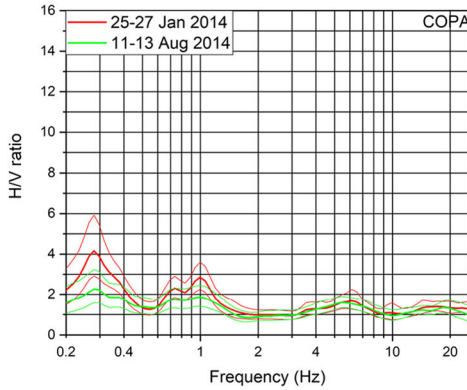
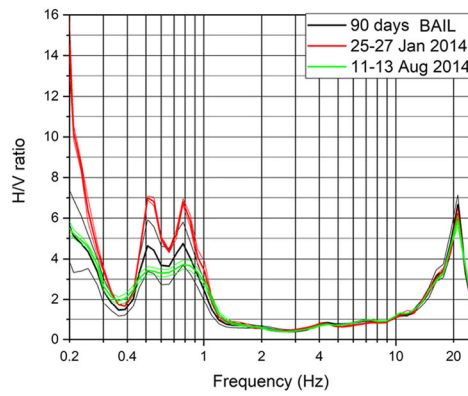
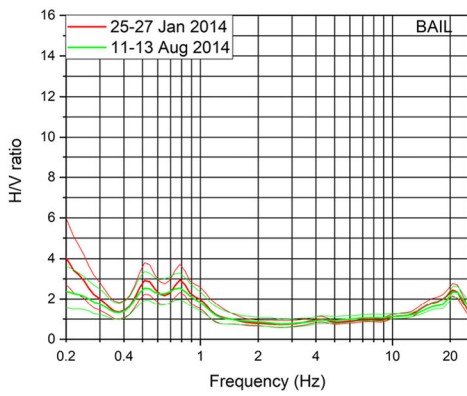
In the previous section, we hinted at the role played by the local structure (i.e., the thickness of the sediments) beneath a station in the variation of the noise level. Many studies (e.g., Nakamura 1989; Parolai et al. 2002) showed the possibility of retrieving information about the seismic response of subsoil by computing the ratio between the spectra of the horizontal and vertical components of ambient seismic noise. This ratio

exhibits a peak associated with the fundamental resonance frequency of a site. The amplitude and sharpness of the peak are a good indicator of the existence of a high shear wave impedance contrast in the subsoil and its frequency depends on the thickness of the layers underneath the station.

In this section, we investigate the influence of the noise variations on the Horizontal-to-Vertical-Noise-Spectral-Ratios (HVNSR) at four stations (BAIL, COPA, EFOR, TIRR) installed on different tectonic environments. The BAIL and COPA stations are located on the thick sediments of the Valah sector of the Moesian Platform while the TIRR and EFOR stations are located on the South-Dobrogean Platform (Mutihac et al. 2007). Manea et al. (2016a, b) mapped the geophysical bedrock in the study area and found the following depths for the station mentioned above: 800 m for BAIL, 660 m for COPA, and 120 m for EFOR. TIRR is located on hard metamorphic rocks constituted of greenschists of Proterozoic age (Raileanu 2006). As input for calculating the HVNSRs, we used the noise data recorded during the same time intervals characterized by different weather conditions in the Black Sea, i.e., from 25th to 27th of January 2014 and 11th to 13th of August 2014.

Figure 10 shows the HVNSRs obtained using the two approaches: the diagrams on the left display the spectral ratios computed using the Geopsy software, while the pictures on the right portray the spectral ratios calculated using the median of the PSD PDFs. The detailed analysis of the results outlines several features. Firstly, the two methods show similar HVNSRs in terms of both shape and frequencies where the resonant peaks occur. For the stations located on deep sediments (BAIL and COPA), resonant peaks are found at lower frequencies ( $< 1$  Hz), while for station EFOR, the fundamental resonant peak is observed at higher frequencies, between 3 and 4 Hz. For the station located on the hard rock (TIRR), the HVNSRs are flat and show no distinct resonance peaks. Secondly, we can notice differences in the HVNSRs computed for the same station. For the BAIL and COPA stations, the amplitude of the low-

**Fig. 10** H/V ratios obtained for BAIL, COPA, EFOR, and TIRR. The left diagrams show the HVNSRs calculated from 100 s length ambient noise windows while the right diagrams indicate the HVNSRs computed from the median PSD PDFs (with red lines for winter period, with green lines for summer period, and with black lines over 90 days)



frequency resonance peaks is larger for the winter interval than for the summer period. These results are important for understanding the increase in the noise levels observed in the period band 2–9 s at stations located on thicker sediments as compared to the sites located on thinner sediments. We consider that the thickness of the sediments also plays a role in the increase of the noise level when the noise sources generate ambient vibrations whose spectral content coincides with the local response. For EFOR, the frequency of the resonance peak shifts from about 4 Hz to approximately 3.4 Hz from winter to summer intervals while the amplitude remains constant. The explanation for this shift could be related to different anthropic noise sources during winter and summer day. The TIRR station also shows a small increase of the HVNSR amplitude at high frequencies when using the noise data recorded during the winter days. Finally, the HVNSRs computed using the median of the PSD PDFs over 90 days seem to average out all the noise variations. Therefore, we can conclude that the HVNSR calculated from the statistics of the PSD PDFs can be used as a proxy to establish whether site effects are present at seismic stations. In addition, the method has several advantages relative to the ‘classical’ one: (i) there is no need to select the data; (ii) the possibility of computing the PSD PDFs over different time intervals from hours to years, and thus the possibility of studying the variation in time of the H/V ratios; (iii) the ease of processing.

## 5 Conclusions

In this paper, we have analyzed ambient noise data recorded between 2012 and 2015 by the seismic stations deployed in the Romanian-Bulgarian cross-border region in order to investigate the characteristics of noise the period range 0.025–10 s. The study was conducted by means of the PSD PDF that proved to be a useful tool to evaluate the seismic noise levels at seismic stations and monitor their performance. At low periods (< 1 s), important diurnal variations, up to 25 dB, are seen at all stations. The observations made at these periods indicate noisy environments for several stations (e.g., EFOR, MANR, RMGR). Good sites for seismic recording of small local events are those with low seismic noise and depend upon to what extent one can minimize the influence of various noise sources. Since one of the main goals of the network installed in the study area is to

record high-quality data, a relocation of these noisy stations should be taken into consideration. At larger periods (2–10 s), the noise power variations are well correlated with season changes, the noise levels being larger during winter and smaller during summer. For stations located far from the Black Sea, the double-frequency peak broadens towards longer periods from summer to winter time. Instead, stations located on the Black Sea coastline show two peaks between 1 and 10 s, one at approximately 2 s and one at around 7 s. The amplitude of the former has been shown to be related to the weather conditions in the Black Sea. The polarization analysis performed also showed that the double-frequency microseisms originating from the Black Sea are dominating during the winter time. We showed that resonance peak amplitude of the noise horizontal to vertical spectral ratios is influenced by the noise variations. For stations located on thick sediments, the low resonance frequency peak has larger amplitudes when noise levels increase due to stormy weather conditions in the Black Sea. We also observed a shift of the fundamental resonance peak from 4 to 3.4 Hz for station EFOR. This shift could be linked to different anthropogenic noise sources during summer and winter periods. Finally, we also suggested that the HVNSR computed from the statistics of PSD PDFs could be used as a proxy to investigate the site conditions.

**Acknowledgments** The authors thank M. Schimmel of Institute of Earth Sciences Jaume Almera, Barcelona, for making available his Time-Frequency Dependent Polarization code and the Geopsy team for providing the Geopsy package. We acknowledge support from/discussions within TIDES COST Action ES1401. We also thank three anonymous reviewers for their constructive comments which significantly improved the paper.

**Funding information** This work was partly supported by a grant of the Romanian National Authority for Scientific Research and Innovation (ANCSI)-UEFISCDI, project number PN-II-RU-TE-2014-4-0701 and partly by a project carried out within Nucleu Program, supported by ANCSI, project number PN 16 35 01 01.

## References

- Bard PY (1999) Microtremor measurements: a tool for site effects estimation? In: Irikura K, Kudo K, Okada H, Sasatani T (eds) The effects of surface geology on seismic motion. Balkema, Rotterdam, 2:1251–1279
- Beucler É, Mocquet A, Schimmel M, Chevrot S, Quillard O, Vergne J, Sylvander M (2015) Observation of deep water microseisms in the North Atlantic Ocean using tide modulations. *Geophys Res Lett* 42(2):316–322
- Boaga J, Vaccari F, Panza GF (2010) Shear wave structural models of Venice Plain, Italy, from time cross-correlation of seismic



- noise. *Eng Geol* 116:189–195. <https://doi.org/10.1016/j.enggeo.2010.09.001>
- Bormann P (2012) Seismic signals and noise. *New manual of seismological observatory practice*
- Brenguier F, Campillo M, Hadziioannou C, Shapiro NM, Nadeau RM, Larose E (2008) Postseismic relaxation along the San Andreas fault at Parkfield from continuous seismological observations. *Science* 321(5895):1478–1481. <https://doi.org/10.1126/science.1160943>
- Bromirski PD, Duennebieer FK, Stephen RA (2005) Mid-ocean microseisms. *Geochem Geophys Geosyst* 6(4):1–19
- Burtin A, Bollinger L, Vergne J, Cattin R, Nabelek JL (2008) Spectral analysis of seismic noise induced by rivers: a new tool to monitor spatiotemporal changes in stream hydrodynamics. *J Geophys Res* 113:B05301. <https://doi.org/10.1029/2007JB005034>
- Cadet H, Macau A, Benjumea B, Bellmunt F, Figueras S (2011) From ambient noise recordings to site effect assessment: the case study of Barcelona microzonation. *Soil Dyn Earthq Eng* 31(3):271–281
- Chevrot S, Sylvander M, Benahmed S, Ponsolles C, Lefevre JM, Paradis D (2007) Source locations of secondary microseisms in western Europe: Evidence for both coastal and pelagic sources. *J Geophys Res Solid Earth* 112:B11
- Chiotoroiu B, Ivanova V, Apostol L (2014) Atmospheric patterns during the storms from January 2014 in Bulgaria and Romania. *Present Environment and Sustainable Development* 8(2):33–44
- Custódio S, Dias NA, Caldeira B, Carrilho F, Carvalho S, Corela C et al (2014) Ambient noise recorded by a dense broadband seismic deployment in western Iberia. *Bull Seismol Soc Am* 104(6):2985–3007
- Diaz J, Villasenor A, Morales J, Pazos A, Cordoba D, Pulgar J, Garcia-Lobon JL, Harnafi M, Carbonell R, Gallart J, Topolberia Seismic Working Group (2010) Background noise characteristics at the IberArray broadband seismic network. *Bull Seismol Soc Am* 100(2):618–628
- Dimitrova L, Solakov D, Simeonova S, Aleksandrova I (2015) System of Earthquakes Alert (SEA) in the Romania-Bulgaria cross border region. *Bulg Chem Commun* 47(B):390–396
- Evangelidis CP, Melis NS (2012) Ambient noise levels in Greece as recorded at the Hellenic Unified Seismic Network. *Bull Seismol Soc Am* 102(6):2507–2517
- Greco B, Neagoe C, Tataru D (2012) Seismic noise characteristics at the Romanian broadband seismic network. *J Earthq Eng* 16(5):644–661
- Greco B, Borleanu F, Tataru D, Zaharia B, Neagoe C (2016) Analysis of Broadband Seismic Noise from Temporary Stations in an Urban Environment, Bucharest, Romania. *International Multidisciplinary Scientific GeoConference SGEM: Surveying Geology & Mining Ecology Management* 3:395–402
- Kislov KV, Gravurov VV, Labuncov M (2010) The analysis of wind seismic noise and algorithms of its determination // *Eos Trans AGU, Fall Meet. Suppl., Abstract S21C-2079*, San Francisco, USA
- Kobayashi N, Nishida K (1998a) Continuous excitation of planetary free oscillations by atmospheric disturbances. *Nature* 395:357–360
- Kobayashi N, Nishida K (1998b) Atmospheric excitation of planetary free oscillations. *J Phys Condens Matter* 10(11):557–11,560
- Konno K, Ohmachi T (1998) Ground motion characteristics estimated from spectral ratio between horizontal and vertical components of microtremors. *Bull Seismol Soc Am* 88(1): 228–241
- Longuet-Higgins MS (1950) A theory of the origin of microseisms. *Philos Trans R Soc* 243:1–35
- Manea EF, Michel C, Poggi V, Fäh D, Radulian M, Balan FS (2016a) Improving the shear wave velocity structure beneath Bucharest (Romania) using ambient vibrations. *Geophys J Int* 207(2):848–861
- Manea EF, Michel C, Fäh D, Cioflan CO (2016b) Mapping the geophysical bedrock of the Moesian Platform using H/V ratios and borehole data. In: *EGU General Assembly Conference Abstracts* 18: 12143)
- Marzorati S, Bindi D (2006) Ambient noise levels in north central Italy. *Geochem Geophys Geosyst* 7(9). <https://doi.org/10.1029/2006GC001256>
- McNamara DE, Boaz RI (2005) Seismic noise analysis system, power spectral density probability density function: stand-alone software package. In: *U. S. geological survey open file report, 2005–1438*. Washington, D.C
- McNamara DE, Buland RP (2004) Ambient noise levels in the continental United States. *Bull Seismol Soc Am* 94:1517–1527
- McNamara DE, Gee L, Benz HM, Chapman M (2014) Frequency-dependent seismic attenuation in the eastern United States as observed from the 2011 central Virginia earthquake and aftershock sequence. *Bull Seismol Soc Am* 104(1):1–18
- Mutihaç V, Stratulat M I, Fechet R M (2007) The geology of Romania. *Didactica si Pedagogica Publishin* 249 pp. (in Romanian)
- Nakamura Y (1989) A method for dynamic characteristics estimation of subsurface using microtremor on the ground surface. *Quarterly Report Railway Technical Research Institute*, 30-1, 25–30
- Oncescu MC, Marza VI, Rizescu M, Popa M (1999) The Romanian earthquake catalogue between 984–1997. In: *Wenzel F, Lungu D (eds) Contributions from the First International Workshop on Vrancea Earthquakes, Bucharest, Romania, November 1–4, 1997*. Kluwer Academic Publishers, Dordrecht, pp 43–48
- Panou AA, Theodulidis N, Hatzidimitriou P, Stylianidis K, Papazchos CB (2005) Ambient noise horizontal-to-vertical spectral ratio in site effects estimation and correlation with seismic damage distribution in urban environment: the case of the city of Thessaloniki (Northern Greece). *Soil Dyn Earthq Eng* 25:261–274
- Papadopoulos GA, Diakogianni G, Fokaefs A, Rangelov B (2011) Tsunami hazard in the Black Sea and the Azov Sea: a new tsunami catalogue. *Nat Hazards Earth Syst Sci* 11:945–963
- Parolai S, Bormann P, Milkereit C (2002) New relationships between vs, thickness of sediments, and resonance frequency calculated by the H/V ratio of seismic noise for the Cologne area (Germany). *Bull Seismol Soc Am* 92(6):2521–2527
- Peterson J (1993) Observations and modeling of background seismic noise, in *U.S. Geological Survey Open-File Report 93–322*, Albuquerque, New Mexico. Schulte-Pelkum,

- Pilz M, Parolai S, Leyton F, Campos J, Zschau J (2009) A comparison of site response techniques using earthquake data and ambient seismic noise analysis in the large urban areas of Santiago de Chile. *Geophys J Int* 178:713–728
- Raileanu V (2006) Annual report for the contract no: 31N/23.01.2006, Project—advanced research of the disaster management of the strong Romanian earthquakes, Director of the project dr. Raileanu V., NIEP
- Rangelov B and Bojkova A (2008) Archaeoseismology in Bulgaria, Proceedings of the International Conference, 29–30 October 2008 Sofia, Publishing House “St. Ivan Rilski”, Sofia, 341–346
- Rastin SJ, Unsworth CP, Gledhill KR, McNamara DE (2012) A detailed noise characterization and sensor evaluation of the North Island of New Zealand using the PQLX data quality control system. *Bull Seismol Soc Am* 102(1):98–113
- Ren Y, Grecu B, Stuart G, Houseman G, Hegedüs E, South Carpathian Project Working Group (2013) Crustal structure of the Carpathian–Pannonian region from ambient noise tomography. *Geophys J Int* 195(2):1351–1369
- Saygin E, Kennett BLN (2008) Ambient seismic noise tomography of Australian continent. *Tectonophysics* 481:116–125. <https://doi.org/10.1016/j.tecto.2008.11.013>
- Schimmel M, Stutzmann E, Arduini F, Gallart J (2011) Polarized Earth’s ambient microseismic noise. *Geochem Geophys Geosyst* 12(7):1–14
- Schulte-Pelkum V, Earle PS, Vernon FL (2004) Strong directivity of ocean-generated seismic noise. *Geochem Geophys Geosyst* (5). <https://doi.org/10.1029/2003GC000520>
- SESAME Project (2004) Guidelines for the implementation of the H/V spectral ratio technique on ambient vibrations measurements, processing and interpretation. [http://sesame-fp5.obs.ujf-grenoble.fr/Papers/HV\\_User\\_Guidelines.pdf](http://sesame-fp5.obs.ujf-grenoble.fr/Papers/HV_User_Guidelines.pdf)
- Shapiro NM, Campillo M, Stehly L, Ritzwoller MH (2005) High resolution surface wave tomography from ambient seismic noise. *Science* 307:1615–1618
- Sheen DH, Shin JS, Kang TS (2009) Seismic noise level variation in South Korea. *Geosci J* 13(2):183–190
- Stutzmann E, Scimmel M, Patau G, Maggi A (2009) Global climate imprint on seismic noise. *Geochem Geophys Geosyst*. <https://doi.org/10.1029/2009GC002619>
- Wegler U, Sens-Schönfelder C (2007) Fault zone monitoring with passive image interferometry. *Geophys J Int* 168(3):1029–1033. <https://doi.org/10.1111/j.1365-246X.2006.03284.x>
- Yang Y, Ritzwoller MH, Levshin AL, Shapiro NM (2007) Ambient noise Rayleigh wave tomography across Europe. *Geophys J Int* 168:259–274
- Zaharia B, Radulian M, Popa M, Grecu B, Bala A, Tataru D (2008) Estimation of the local response using Nakamura method for Bucharest area. *Rom Rep Phys* 60(1):131–144